

Int. Workshop on Heavy Quarks and Leptons
Vietri sul Mare, Italy, May 27 - June 1, 2002

CHIRAL DYNAMICS and $B \rightarrow 3\pi$ DECAY

Ulf-G. Meißner

Forschungszentrum Jülich, Institut für Kernphysik (Theorie)

D-52425 Jülich, Germany

and

Karl-Franzens Universität Graz, Institut für Theoretische Physik

A-8010 Graz, Austria

ABSTRACT

I discuss our knowledge of the scalar sector of QCD and how it impacts the determination of the CKM angle α from the isospin analysis of $B \rightarrow \rho\pi$ decay.

1 Introduction and motivation

CP violation has been established experimentally in the K- and B-meson systems. In the Standard Model, this can be explained in terms of one single phase, which leads to complex entries in the CKM matrix. The unitarity of this matrix may be represented in terms of various triangles, one of them to be measured at the B-factories. Any violation of unitarity would be a signal of physics beyond the Standard Model. However, to achieve the required accuracy to really test the relation $\alpha + \beta + \gamma = \pi$, where α, β , and γ are the three

angles of the triangle, one has to be able to precisely calculate or eliminate the final-state interactions (FSI) of the mesons generated in the various B-decays (more precisely, it is the strong phase generated by the FSI associated with diagrams of the “wrong” weak phase that pose especial difficulty). Here, we will be concerned with the decay $B \rightarrow 3\pi$, because the isospin analysis possible in $B \rightarrow \rho\pi$ decay allows to extract $\sin(2\alpha)$ ^{1, 2)}. Recent observations, however, have triggered the question about a possible “hadronic pollution” in the $\rho\pi$ phase space. In particular, the E791 collaboration has found that half of the rate of $D^- \rightarrow \pi^- \pi^+ \pi^-$ decay goes via the $D^- \rightarrow \pi^- \sigma(500) \rightarrow \pi^- \pi^+ \pi^-$ doorway state ³⁾. This measurement was also considered as further evidence for a light scalar–isoscalar meson, the elusive σ . Furthermore, it was shown in ref. ⁴⁾ that the inclusion of this channel can improve the theoretical description of the ratio

$$\mathcal{R} = \frac{\text{Br}(\bar{B}^0 \rightarrow \rho^\mp \pi^\pm)}{\text{Br}(B^- \rightarrow \rho^0 \pi^-)} = 2.7 \pm 1.2, \quad (1)$$

measured at CLEO and BABAR. Note that $\mathcal{R} \simeq 6$ at tree level in naive factorization. Since there is on-going debate about the nature of the σ , we will address here the following questions:

- * What do we know about the scalar sector of QCD?
- * What is its impact on $B \rightarrow \rho\pi$ decay?

2 The scalar sector of QCD

The scalar–isoscalar sector of QCD is highly interesting because of its vacuum quantum numbers, and its direct relation to the quark mass terms (explicit chiral symmetry breaking), the related σ -terms, and so on. Its most distinct characteristics are the very strong final-state interactions, signaled e.g. by the rapidly rising isospin zero, S-wave $\pi\pi$ phase shift $\delta_0^0(s)$ or the observation that the scalar pion radius, $\langle r_S^2 \rangle_\pi \simeq 0.6 \text{ fm}^2$, is sizeably bigger than the corresponding vector (charge) radius, $\langle r_V^2 \rangle_\pi \simeq 0.4 \text{ fm}^2$. Note also that there is no direct experimental probe with such quantum numbers. Therefore, theoretical investigations using different tools have been employed to deepen our understanding of this sector, these are Chiral Perturbation Theory (CHPT), resummation schemes consistent with CHPT, unitarity, analyticity, ... (like e.g. the chiral

unitary approach ⁵⁾) and also dispersion relations. The following general results emerge: First, a **consistent** picture of the scalar (pion and kaon) form factors is obtained, and, second, all the light (non-strange and strange) scalar mesons are dynamically generated in a large class of resummation schemes (see e.g. ref. ⁶⁾), although this later topic is still vigorously debated¹. For the impact on the $B \rightarrow \rho\pi$ decay, we fortunately only need the (non-strange) scalar form factor of the pion, $\Gamma_\pi(s)$ (or, equivalently, the $\sigma \rightarrow \pi\pi$ vertex function $\Gamma_{\sigma\pi\pi}(s)$), defined via

$$\langle 0 | \hat{m}(\bar{u}u + \bar{d}d) | \pi^a(p) \pi^b(p') \rangle = \delta^{ab} M_\pi^2 \Gamma_\pi(s) = \mathcal{N} \Gamma_{\sigma\pi\pi}(s) , \quad s = (p + p')^2 . \quad (2)$$

The scalar form factor is shown in fig. 1 for the various theoretical approaches mentioned above. We will use here the result of the chiral unitary approach ⁷⁾, which was successfully tested e.g. in $J/\Psi \rightarrow \phi\pi\pi(\bar{K}K)$ decays. It is worth to point out that the scalar form factor constructed in ⁷⁾ is systematically matched to the CHPT representation, and it embodies by construction the coupled channel $\pi\pi/\bar{K}K$ dynamics. It is also consistent with the dispersive results of ref. ⁸⁾. Most importantly for the later discussion, we remark that the form of the pion scalar form factor is very different from a Breit-Wigner (BW) form with a running width, as used e.g. in ³⁾, compare fig. 2. This apparent difference casts doubt on the recent conclusions of refs. ^{3, 4)}. The situation is completely different for the pion vector form factor entering the $\rho\pi$ intermediate state - it can be described to good precision by a BW with running width. More generally, the vector form factor can be reconstructed from unitarity and analyticity and matched to CHPT. The resulting vertex function does not differ significantly from a BW with running width (see ref. ⁹⁾ for a detailed discussion on this point and corresponding figures).

3 Extending the isospin analysis of $B \rightarrow \rho\pi$ decay

Next, we wish to consider the impact of the $\sigma\pi$ channel on the isospin analysis of $B \rightarrow \rho\pi$. Since in the initial state the B-meson has isospin $I_i = 1/2$, and the final state $\rho\pi$ system has $I_f = 0, 1, 2$, transitions with $|\Delta I| = 1/2, 3/2, 5/2$

¹Consequently, by “ σ ” we always mean a two-pion state with total isospin zero and in a relative S-wave state, $(\pi\pi)_S$, understanding its dynamical origin in the strong pionic FSI for these quantum numbers.

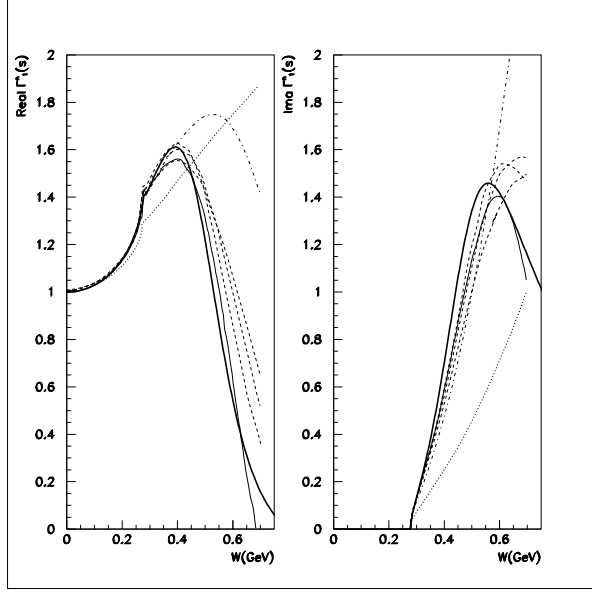


Figure 1: *Real (left) and imaginary part (right) of the non-strange scalar form factor of the pion. Solid line: chiral unitary approach as discussed in the text, dotted/dash-dotted line: CHPT to one/two loops, dashed line: dispersive results.*

are possible. If one parameterizes the corresponding amplitudes $a_{bc} \equiv A(B^0 \rightarrow \rho^b \pi^c)$ (with $a, b = \{+, 0, -\}$) by $A_{|\Delta I|, I_f}$, one gets

$$\begin{aligned}
 a_{+-} &= \frac{1}{2\sqrt{3}} [A_{3/2,2} + A_{5/2,2}] + \frac{1}{2} [A_{3/2,1} + A_{1/2,2}] + \frac{1}{\sqrt{6}} A_{1/2,0} , \\
 a_{-+} &= \frac{1}{2\sqrt{3}} [A_{3/2,2} + A_{5/2,2}] - \frac{1}{2} [A_{3/2,1} + A_{1/2,2}] + \frac{1}{\sqrt{6}} A_{1/2,0} , \\
 a_{00} &= -\frac{1}{\sqrt{3}} [A_{3/2,2} + A_{5/2,2}] + \frac{1}{\sqrt{6}} A_{1/2,0} ,
 \end{aligned} \tag{3}$$

noting that $A(B^0 \rightarrow \pi^+ \pi^- \pi^0) = f_+ a_{+-} + f_- a_{-+} + f_0 a_{00}$, where f_i is the form factor describing $\rho^i \rightarrow \pi\pi$. Because of CKM unitarity, there are two independent weak phases, a possible choice being

$$\frac{V_{ub}^* V_{ud}}{|V_{ub}^* V_{ud}|} = \exp(i\gamma) , \quad \frac{V_{tb}^* V_{td}}{|V_{tb}^* V_{td}|} = \exp(-i\beta) , \quad \alpha = \pi - \beta - \gamma , \tag{4}$$

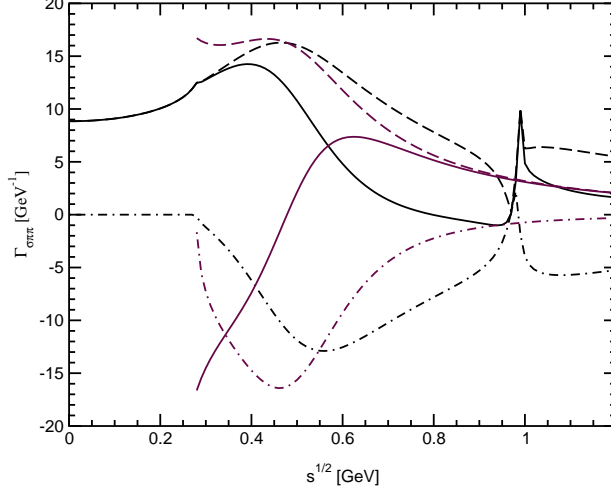


Figure 2: The $\sigma \rightarrow \pi^+(p_+)\pi^-(p_-)$ form factor $\Gamma_{\sigma\pi\pi}$ as a function of \sqrt{s} , with $s = (p_+ + p_-)^2$. The real (solid line) and imaginary (dot-dashed line) parts of $\Gamma_{\sigma\pi\pi}$, as well as its modulus (dashed line), are shown. The curves which do not persist below physical threshold, $\sqrt{s} = 2M_\pi \sim 0.27$ GeV, correspond to the form factor adopted in Ref. ⁴⁾, whereas the curves which extend to $s = 0$ correspond to the form factor adopted here ⁷⁾. Both representations are normalized that their real parts agree at $\sqrt{s} = 0.478$ GeV.

leading to

$$\begin{aligned} e^{i\beta} a_{+-} &= T^{+-} e^{-i\alpha} + P^{+-} , \\ e^{i\beta} a_{-+} &= T^{-+} e^{-i\alpha} + P^{-+} , \\ e^{i\beta} a_{00} &= T^{00} e^{-i\alpha} + P^{00} , \end{aligned} \quad (5)$$

from which $\sin(2\alpha)$ can be deduced, having made the crucial assumption that the penguin is $|\Delta I| = 1/2$, so that

$$P^{00} = \frac{1}{2}(P^{+-} + P^{-+}) . \quad (6)$$

With this penguin assumption, one has 10 parameters, which can all be determined from a Dalitz plot analysis. As discussed in ref. ⁹⁾, there are three different sources of isospin violation (IV) that could invalidate this analysis:

1) IV generates an additional amplitude of $|\Delta I| = 5/2$ character, 2) IV can distinguish the f_i , and 3) IV can generate penguins with $|\Delta I| = 3/2$. Some of these effects can be mitigated in an empirically driven way, as long as $A_{5/2,2}$ and $A_{3/2,2}$ share the same weak phase. However, non- $|\Delta I| = 1/2$ penguin effects, be they electroweak penguin contributions or contributions consequent to isospin-violating effects in the hadronic matrix elements of $|\Delta I| = 1/2$ operators, present an irreducible hadronic ambiguity from the viewpoint of this analysis (for a more detailed discussion, see ref. ⁹⁾). Note that this is quite different to the isospin analysis of $B \rightarrow \pi\pi$ decay ¹⁰⁾. Returning to the scalar sector, we remark that $\sigma\pi$ contributes preferentially to the $\rho^0\pi^0$ final state and thus can break the assumed penguin relation. However, $B \rightarrow \sigma\pi$ has definite transformation properties under CP, so that an extended isospin analysis is possible. Defining $a_{00}^\sigma = A(B^0 \rightarrow \sigma\pi^0)$, we have

$$e^{i\beta} a_{00}^\sigma = T_\sigma^{00} e^{-i\alpha} + P_\sigma^{00}. \quad (7)$$

T_σ^{00} and P_σ^{00} are unrelated to the parameters of Eq. (5), so that we gain four additional hadronic parameters. However, more observables are present as well. Including the scalar channel, we now have $A_{3\pi} \equiv A(B^0 \rightarrow \pi^+\pi^-\pi^0) = f_+ a_{+-} + f_- a_{-+} + f_0 a_{00} + f_\sigma a_{00}^\sigma$, where f_σ is the form factor describing $\sigma \rightarrow \pi^+\pi^-$. For this extended analysis to be useful, the σ has to contribute significantly to B^0, \bar{B}^0 decay. It is worth noting that any discernable presence of the $B \rightarrow \sigma\pi$ channel in the $B \rightarrow \rho\pi$ phase space falsifies the notion that the “nonresonant” background can be characterized by a single, constant phase across the Dalitz plot ¹¹⁾.

4 Evaluating $B \rightarrow \rho\pi$ in the presence of the $\sigma\pi$ channel

Our starting point is the effective $|\Delta B| = 1$ Hamiltonian for $b \rightarrow dq\bar{q}'$ decay

$$\mathcal{H}_{\text{eff}} = \frac{G_F}{\sqrt{2}} \left[\sum_{j=u,c} \lambda_j \left(C_1 O_1^j + C_2 O_2^j \right) - \lambda_t \sum_{i=3}^{10} C_i O_i \right], \quad (8)$$

with $\lambda_q = V_{qb} V_{qq}^*$, V_{ij} an element of the CKM matrix and the operators are ordered such that the Wilson coefficients obey $C_1 \sim O(1)$, $C_1 > C_2 \gg C_{3,\dots,10}$. We evaluate the resonance contributions to $B \rightarrow 3\pi$ decay by using a product

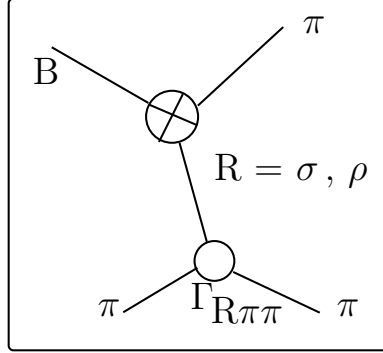


Figure 3: *Generic diagram for $B \rightarrow R\pi \rightarrow 3\pi$ decay, where $\Gamma_{R\pi\pi}$ denotes the corresponding strong vertex function, $R = \sigma, \rho$. The crossed vertex symbolizes the weak $B \rightarrow R\pi$ transition.*

ansatz, see fig. 3. For the requisite amplitudes, this means

$$A_R(B \rightarrow \pi^+\pi^-\pi) = \langle (R \rightarrow \pi^+\pi^-\pi) | \mathcal{H}_{\text{eff}} | B \rangle = \underbrace{\langle R\pi | \mathcal{H}_{\text{eff}} | B \rangle}_{\text{m.e.}} \underbrace{\Gamma_{R \rightarrow \pi\pi}}_{\text{v.f.}}, \quad (9)$$

where we compute the matrix element (m.e.) in factorization (including penguins) in the same way it was done in refs. ^{4, 12)} for a crisp comparison (detailed formulae can be found in ref. ⁹⁾). To ascertain the impact of the $B \rightarrow \sigma\pi$ channel to $B \rightarrow \rho\pi$ decay, we combine the decay channels at the amplitude level, $\mathcal{M} = A_\sigma(B \rightarrow \pi^+\pi^-\pi) + A_\rho(B \rightarrow \pi^+\pi^-\pi)$, and then integrate over the relevant three-body phase space to compute the effective $B \rightarrow \rho\pi$ branching ratios. The main new ingredient is the vertex function (v.f.) for which we employ in the $\sigma\pi$ channel the scalar form factor discussed earlier and for the $\rho\pi$ mode the vector form factor from ref. ¹³⁾. In table 1 we display the effective branching ratios for $B \rightarrow \rho\pi$ decay computed at tree level (and also including penguins following ref. ¹²⁾). We find that at tree level $\mathcal{R} \simeq 5.5$, and the inclusion of penguin contributions lowers this value to $\mathcal{R} \simeq 5.1$. Neither this ratio nor the calculated branching ratios depend in any significant way on the various vector form factors employed. The $B \rightarrow \sigma\pi$ branching ratios are collected in table 2. The computed values of $\mathcal{R} \simeq 2.0 \dots 2.6$ are consistent with the empirical value of $\mathcal{R}_{\text{exp}} = 2.7 \pm 1.2$, albeit the errors are large. The reduction in \mathcal{R} is mostly due to the effect of the $\sigma\pi$ channel on the B^- decay

Table 1: *Effective branching ratios (in units of 10^{-6}) for $B \rightarrow \rho\pi$ decay, computed at tree level. The numbers in parentheses include penguin contributions as well, after ref. ¹²⁾. “BW” denotes the use of the form factors of refs. ^{4, 12)}, whereas “RW” denotes the use of the vector form factor of ref. ¹⁴⁾. Finally, “*” denotes the use of the form factor advocated here ⁹⁾.*

δ [MeV] (f.f.)	$\bar{B}^0 \rightarrow \rho^- \pi^+$	$\bar{B}^0 \rightarrow \rho^+ \pi^-$	$\bar{B}^0 \rightarrow \rho^0 \pi^0$	$B^- \rightarrow \rho^0 \pi^-$
200 (BW)	15.1 (14.7)	4.21 (4.24)	0.508 (0.497)	3.50 (3.68)
300 (BW)	16.4 (16.0)	4.74 (4.76)	0.918 (0.908)	3.89 (4.10)
200 (RW)	15.1 (14.8)	4.19 (4.21)	0.468 (0.463)	3.49 (3.68)
300 (RW)	16.4 (16.0)	4.69 (4.70)	0.835 (0.831)	3.87 (4.07)
200 (*)	15.3 (14.9)	4.26 (4.28)	0.473 (0.467)	3.49 (3.68)
300 (*)	16.4 (16.0)	4.75 (4.76)	0.865 (0.859)	3.85 (4.06)
δ [MeV] (f.f.)	$B^0 \rightarrow \rho^+ \pi^-$	$B^0 \rightarrow \rho^- \pi^+$	$B^0 \rightarrow \rho^0 \pi^0$	$B^+ \rightarrow \rho^0 \pi^+$
200 (BW)	15.1 (14.7)	4.21 (4.15)	0.508 (0.615)	3.50 (3.68)
300 (BW)	16.4 (16.0)	4.74 (4.67)	0.918 (1.02)	3.89 (4.10)
200 (RW)	15.1 (14.7)	4.19 (4.13)	0.468 (0.571)	3.49 (3.68)
300 (RW)	16.4 (15.9)	4.69 (4.62)	0.835 (0.935)	3.87 (4.07)
200 (*)	15.3 (14.8)	4.26 (4.20)	0.473 (0.576)	3.49 (3.68)
300 (*)	16.4 (15.9)	4.75 (4.68)	0.865 (0.963)	3.85 (4.06)

Table 2: Effective branching ratios (in units of 10^{-6}) for $B \rightarrow \sigma\pi$ and $B \rightarrow \rho\pi$ decay, computed at tree level. The form factors are defined as in Table 1.

δ (f.f.) [MeV]	$B^- \rightarrow \sigma\pi^-$	$B^- \rightarrow (\rho^0 + \sigma)\pi^-$	$\bar{B}^0 \rightarrow \sigma\pi^0$	$\bar{B}^0 \rightarrow (\rho^0 + \sigma)\pi^0$	\mathcal{R}
200 (BW)	2.97	6.16	0.0258	0.516	3.1
300 (BW)	5.17	8.61	0.0457	0.940	2.5
200 (RW)	2.97	6.19	0.0258	0.475	3.1
300 (RW)	5.17	8.62	0.0457	0.855	2.4
200 (*)	4.11	7.61	0.0396	0.508	2.6
300 (*)	7.01	10.7	0.0663	0.916	2.0

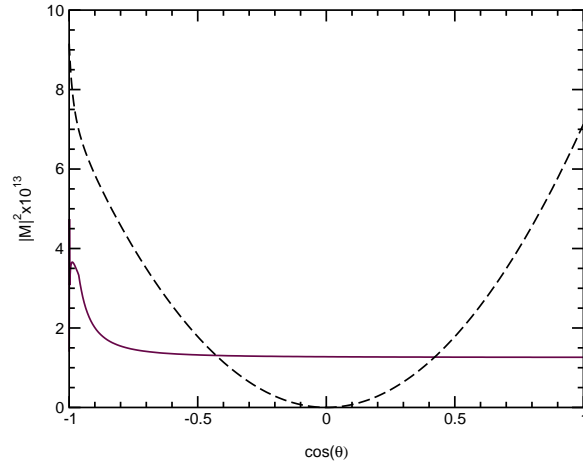


Figure 4: Absolute square of the matrix element, $|M|^2$, for $B^- \rightarrow \rho^0 \pi^-$ decay (dashed line), and for $B^- \rightarrow \sigma \pi^-$ decay (solid line), as a function of $\cos \theta$ at $t = M_\rho^2$.

mode. Turning to $B \rightarrow \sigma \pi^0$ decay, we see that the contribution of the σ meson to $B^0(\bar{B}^0) \rightarrow \rho \pi$ decay is *much* smaller — with the scalar form factor we advocate, the effect is some 10%. Interestingly the σ has a tremendous impact on $B^- \rightarrow \rho^0 \pi^-$ decay (very similar to the large effect in $D^- \rightarrow \pi^+ \pi^- \pi^-$), and a relatively modest one on $\bar{B}^0 \rightarrow \rho^0 \pi^0$ decay. Let us emphasize that we have realized our numerical analysis at tree level, so that the precise numbers but not the trends will change when a more refined analysis is performed. It is the relative size of the penguin contributions in $\bar{B}^0 \rightarrow \sigma \pi^0$ and $\bar{B}^0 \rightarrow \rho^0 \pi^0$ decay which is of relevance to the isospin analysis to extract $\sin(2\alpha)$. The presence of the $\sigma \pi^0$ final state in the $\rho^0 \pi^0$ phase space can break the assumed relationship, Eq. (6), between the penguin contributions in $\rho \pi$ and thus mimic the effect of isospin violation — alternatively we can expand the $\rho \pi$ analysis to include the $\sigma \pi$ channel. It is worth noting that the $\sigma \pi^0$ and $\rho^0 \pi^0$ contributions can, to some measure, be distinguished. Certainly the $\sigma \pi^0$ and $\rho \pi^0$ contributions behave differently under the cut on the invariant mass of the $\pi^+ \pi^-$ pair. Moreover, making a cut on the helicity angle θ , ought also be helpful in separating the ρ^0 and σ contributions. This is illustrated in fig. 4 for $B^- \rightarrow \rho^0 / \sigma \pi^-$. The $\rho^0 \pi$ contributions roughly follow a $\cos^2(\theta)$ distribution,

whereas the $\sigma\pi$ contributions are quite flat, save for the bump resulting from the u-channel contribution $\sim \Gamma_{\sigma\pi\pi}(u)$. Cutting on the helicity angle θ should also help disentangle the contributions from some of the intermediate B^* and B_0 resonances. Such type of terms were claimed to be of importance in ref. ¹²⁾. The contributions of these non-resonant intermediate states to the $\rho\pi$ channels has recently been scrutinized in ref. ¹⁵⁾, where it was shown that the energy dependence of the intermediate heavy-meson propagator can lead to a drastic suppression of such contributions and thus the lowering of the value for \mathcal{R} due to the σ persists in such a refined analysis. We also point out that an additional contribution to the phenomenological value of \mathcal{R} , realized through a diagram mediated by the $a_1^-(1260)$ meson, is proposed in ref. ¹⁶⁾ (it might turn out to be insignificant in a more refined analysis for the same reasons just discussed for the B^* 's).

5 Summary and outlook

In this paper, we have scrutinized the role of the σ meson in $B \rightarrow \rho\pi \rightarrow 3\pi$ decay, understanding its dynamical origin in the strong pion-pion final state interactions in the scalar-isoscalar channel. The presence of the $\sigma\pi^0$ contribution in the $\rho^0\pi^0$ phase space is important in that it can break the assumed relationship between the penguin amplitudes, Eq. (6), consequent to an assumption of isospin symmetry. In this, then, its presence mimics the effect of isospin violation. The salient results of our investigation can be summarized as follows:

- i) We have considered how SM isospin violation can impact the analysis to extract α in $B \rightarrow \rho\pi$ decay. Under the assumption that $|\Delta I| = 3/2$ and $|\Delta I| = 5/2$ amplitudes share the same weak phase, the presence of an additional amplitude of $|\Delta I| = 5/2$ character, induced by isospin-violating effects, does not impact the $B \rightarrow \rho\pi$ analysis in any way. This is in contradistinction to the isospin analysis in $B \rightarrow \pi\pi$. Thus the isospin-violating effects of importance are those which can break the assumed relationship between the penguin contributions, Eq. (6).
- ii) The scalar form factor can be determined to good precision by combining the constraints of chiral symmetry, analyticity, and unitarity. The form factor we adopt describes the appearance of the $f_0(980)$ as well, so that

the shape of the $f_0(980)$ contribution in $B \rightarrow f_0(980)\pi \rightarrow 3\pi$, e.g., should serve as a test of our approach. We emphasize that the resulting scalar form factor is very different from the commonly used Breit-Wigner form with a running width. This is in stark contrast to the vector form factor, which is dominated by the ρ resonance. In that case, one can construct simple forms that fit the theoretical and empirical constraints.

- iii) Remarkably, the impact of the $\sigma\pi$ channel on the ratio \mathcal{R} , cf. Eq. (1), is huge. The numbers we find for \mathcal{R} are in agreement with the empirical ones, given its sizeable experimental uncertainty. This underscores the suggestion made, as well as improves the calculations done, in Ref. ⁴⁾. Our analysis is based on *consistent* scalar and vector form factors. This conclusion persists if one includes non-resonant B^* , B_0 intermediate states ¹⁵⁾.
- iv) On the other hand, the impact of the $\sigma\pi$ channel on the $B \rightarrow \rho\pi$ isospin analysis is merely significant. Varying the cuts on the $\pi\pi$ invariant mass and helicity angle θ should be helpful in disentangling the various contributions.
- v) We have shown that one can expand the isospin analysis to include the $\sigma\pi$ channel because it has definite properties under CP. This may be necessary if varying the cuts in the $\pi\pi$ invariant mass and helicity angle θ are not sufficiently effective in suppressing the contribution from the $\sigma\pi^0$ channel in the $\rho^0\pi^0$ phase space.

This work is merely a first step in exploiting constraints from chiral symmetry, analyticity, and unitarity in the description of hadronic B decays. In particular, the contribution of the “doubly” OZI-violating strange scalar form factor and its phenomenological role in factorization breaking ought be investigated.

Acknowledgements

I am grateful to Susan Gardner for a very pleasant collaboration on the topics reported here and José Antonio Oller and Jusak Tandean for useful comments. I thank the organizers for their invitation and superbe organization.

References

1. H. J. Lipkin, Y. Nir, H. R. Quinn, and A. Snyder, Phys. Rev. D **44**, 1454 (1991).
2. A. E. Snyder and H. R. Quinn, Phys. Rev. D **48**, 2139 (1993).
3. M. Aitala *et al.* [E791 Collaboration], Phys. Rev. Lett. **86**, 770 (2001).
4. A. Deandrea and A. D. Polosa, Phys. Rev. Lett. **86**, 216 (2001).
5. J. A. Oller, E. Oset, and A. Ramos, Prog. Part. Nucl. Phys. **45**, 157 (2000).
6. M. Jamin, J. A. Oller, and A. Pich, Nucl. Phys. B **587**, 331 (2000).
7. Ulf-G. Meißner and J. A. Oller, Nucl. Phys. A **679**, 671 (2001).
8. J. F. Donoghue, J. Gasser, and H. Leutwyler, Nucl. Phys. B **343**, 341 (1990).
9. S. Gardner and Ulf-G. Meißner, Phys. Rev. D **65**, 094004 (2002).
10. S. Gardner, Phys. Rev. D **59**, 077502 (1999).
11. J. Charles, A. Le Yaouanc, L. Oliver, O. Pene, and J. C. Raynal, Phys. Lett. B **425**, 375 (1998); **433**, 441(E) (1998).
12. A. Deandrea, R. Gatto, M. Ladisa, G. Nardulli, and P. Santorelli, Phys. Rev. D **62**, 036001 (2000).
13. S. Gardner and H. B. O’Connell, Phys. Rev. D **57**, 2716 (1998); **62**, 019903(E) (1998).
14. P. F. Harrison and H. R. Quinn [BABAR Collaboration], editors, “The BaBar physics book: Physics at an asymmetric B factory,” SLAC-R-0504.
15. J. Tandean and S. Gardner, arXiv:hep-ph/0204147.
16. N. Paver and Riazuddin, arXiv:hep-ph/0107330.